Fluorescent Fingerprinting of Molecular Recognition Landscapes**

Manfred Auer,* Christine Graf, and James J. La Clair*

Within the last decade, the number of molecules examined per experiment has dramatically increased. This advance now allows molecular matter to be screened on an unprecedented scale, and has, for a large part, allowed the completion of expansive projects, such as the sequencing of the genomes of over 30 organisms.[1] The next advance lies in putting these advances in a *popular* format, thereby extending a common medium for molecular information. While technologies, such as DNA microarraying,[2] begin to reach this level, by accessing up to 10^6 different molecular recognition events, considerable hurdles exist before these and related multidimensional technologies can identify a single molecular component in array of materials with similar structural and/or biophysical features.

Multidimensional screening has become possible as a result of the development of: 1) spatially addressable microarrays,[2] 2) more responsive sensing elements (i.e., single molecule spectroscopy),[3] 3) molecular encoding,[4] 4) "molecular noses"[5] and/or 5) microrobotics.[6] Currently, a significant portion of these advances employ fluorescence spectroscopy.

For a large part, fluorescent methodologies are based on monitoring steady-state fluorescent probes (i.e., compounds whose rigid structural backbone provides a maximum fluorescence with minimal wavelength dependency). In contrast, the SENSI-like fluorophore (**1**), in which rotation about six bonds is possible, has numerous conformations both in the ground and excited states.[7] Each conformation presents a different extent of conjugation, and therefore, increases the information density expressed within this probe's absorption and emission spectra. The complex photophysics of this system[8] provide information density far greater than that of traditional rigid fluorophores (e.g., fluorescein and rhodamine).

The restriction of the space about **1** upon contact with, or approach to, the surface of another molecule or group of molecules can alter access to various charge transfer states or conformers, thereby reducing the net photophysical response.[8] This information provides a rich medium to differentiate molecular recognition events. Herein, we illustrate how this tool can be used to distinguish low-affinity molecular recognition events. A typical class of carbohydrate–protein interactions is used as a model system.

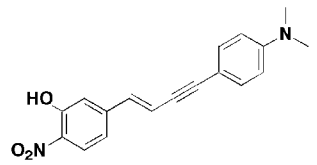

SENSI **1**

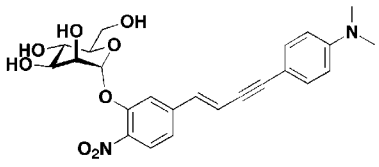

2

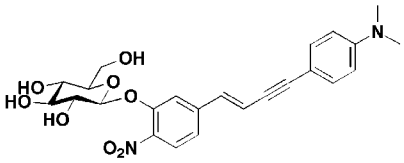

3

Agglutinins from *Lens culinaris* (LCA),[9] *Galanthus nivalis* (GNL),[10] and *Pisum sativum* (PSA)[11] share a common recognition of α-mannosides,[12] but have no affinity towards β-glucosides. Lectins LCA and PSA are homodimeric proteins consisting of an α and β chain, they are 91 % homologous and have comparable three-dimensional structures. Like other legume lectins two large antiparallel β-sheets stretch out over the whole dimer and one calcium and one manganese atom lie in the vicinity of the carbohydrate recognition site.[9, 11] Dimeric complexes of LCA and PSA contain four possible carbohydrate binding sites.

In contrast to LCA and PSA, the tetrameric GNL agglutinin belongs to the super-family of α-D-mannose-specific plant-bulb lectins known to be potent inhibitors of retroviruses. The crystal structure of this lectin complexed with methyl α-D-mannose reveals a novel β-sheet polypeptide fold having threefold symmetry. Three antiparallel four-strand β-sheets, each with a conserved mannose-binding site, are arranged as a 12-strand β-barrel. Pairs of monomers form stable dimers through C-terminal strand exchange. The hybrid β-sheets so formed are the sites for high-affinity mannose binding at or on the dimer interface. Occupancy observed at corresponding sites in other β-sheets suggests that there could be twelve binding sites per tetramer.[10]

A series of carbohydrate ligands was prepared by attaching the phenolic group in **1** to the anomeric center of a given carbohydrate.[12] Using this connection, carbohydrates representing active-binding α-mannoside **2**[12] and nonbinding β-glucoside **3** were prepared using a previously described phase-transfer method.[7] Even using the maximum sensitivity of our spectrometer,[13] fluorescence arising from aqueous solutions of **1**–**3** could not be resolved from the background when examined over an excitation range from $\lambda_a = 350$ to 450 nm and emission range from $\lambda_e = 480$ to 600 nm.[13] Fluorescence from the label **1** became detectable only after mixing with a lectin.

[*] Univ.-Doz. Dr. M. Auer, C. Graf
Allergic Diseases Unit
Fluorescence based HTS-Technology Program
Novartis Forschungsinstitut GmbH
Brunner Strasse 59, 1235 Vienna (Austria)
Fax: (+43) 1-86634-727
E-mail: manfred.auer@pharma.novartis.com
Dr. J. J. La Clair
Bionic Brothers
Postfach 511107, 13371 Berlin (Germany)
E-mail: bionicbros@yahoo.com

[**] J.J.L. thanks Wolfgang Rettig (Humboldt University) for his generosity during the preparation of this manuscript and the Uebbing Foundation for support. M.A. thanks Jan E. de Vries for continuous support and encouragement.

  1433-7851/01/4010-1889 $ 17.50+.50/0

As presented in the upper right corner of Figure 1a, only mixtures containing **2** and a lectin fluoresced upon excitation at $\lambda_a = 370$ nm. By using a conventional two-dimensional

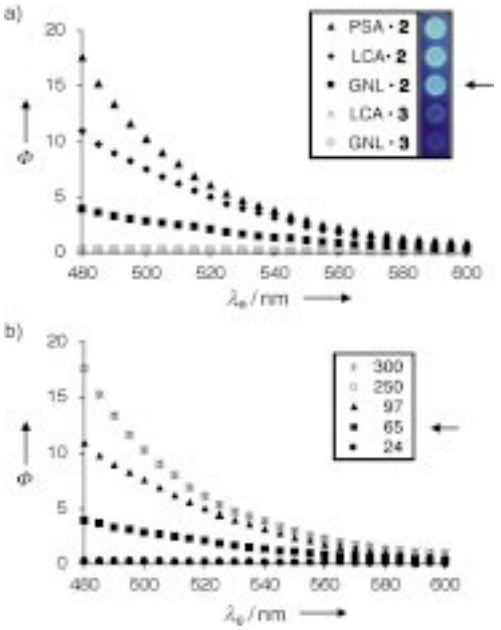

Figure 1. Fluorescence emission spectra from the complex of the conjugated carbohydrates **2** and **3** with lectins PSA, LCA, and GNL. Spectra provided are given by plotting intensity (Φ) versus emission wavelength (λ_e) at a given excitation wavelength ($\lambda_a = 370$ nm). a) Incubation of lectin at 300 μM with carbohydrate at 200 μM. The upper right section shows which wells fluoresce. The relative intensity is given by PSA · **2** > LCA · **2** > GNL · **2** ≫ LCA · **3** ∼ GNL · **3**. b) Titration of 200 μM of **2** with PSA. the spectral information found in (a) can be reproduced by using the same spectral settings and altering the concentration of PSA from 24 to 300 μM in a stepwise manner. Note that spectra highlighted by arrows (i.e., 300 μM of GNL with 200 μM **2** and 65 μM of PSA with 200 μM **2**) are nearly indistinguishable.

approach, we would conclude that lectins PSA, LCA, and GNL bind to **2** and not to **3**. Each of these interactions could then be identified by plotting fluorescence intensity (Φ) versus emission wavelength (λ_e), as illustrated by the five spectra displayed in Figure 1a. For this method to be valid, one must certify that the observed effects can not be produced by alteration of the stoichometry of the complex. As seen in Figure 1b, a comparable series of spectra were produced by mixing **2** with PSA. Comparing the trials in Figure 1 highlighted by arrows, the fluorescence arising from incubating 65 μM PSA with 200 μM **2** is nearly indistinguishable from that of **2** with 300 μM GNL (squares in Figure 1b and Figure 1a, respectively).

Advantageously, the response from **1** was dependent on the choice of *both* excitation and emission wavelength. Data was collected in a three-dimensional manner and plotted in projection or contour (Figure 2). These topographies illustrate a simple means to fluorescently "landscape" molecular recognition. The addition of LCA and PSA to **2** resulted in comparable responses (Figure 2a–c), displaying only modest alteration in the fluorescence intensity observed around an excitation at $\lambda_a = 410$ nm and emission at $\lambda_e = 505$ nm.[14] The structurally different lectin GLN bound to **2**, presented a different topology (Figure 2d), including a second maximum at $\lambda_a = 413$ nm and $\lambda_e = 490$ nm. Landscapes arising from mannoside **2** (Figure 2b–d) differ from those obtained with the nonbinding carbohydrate **3** (Figure 2e, f). Nonspecific multiple binding site interactions with **3** were easily distinguished by examining the relative fluorescence in the region between $\lambda_a = 420$ nm and 440 nm (excitation) and $\lambda_e = 520$ nm and 570 nm (emission).

As illustrated by comparison of Figure 2b or 2c with 2d, landscapes from ligand **2** served to resolve PSA or LCA from GLN. On the other hand, landscapes generated under identical conditions with the nonspecific binding **3** did not distinguish between the two classes of agglutinins (Figure 2e and 2f) because the structure of these landscapes was inconsistent, deviating by up to 40% at each data point even after repeated measurements. While this discrepancy primarily arose from the increased background associated with the reduced fluorescence intensity (Figure 2h), other nonspecific interactions (i.e., mixing **1**–**3** with bovine serum albumin, BSA) gave comparable inconsistent data sets.[15]

Most importantly, this three-dimensional method provides a means to distinguish recognition events from stoichiometric effects. As illustrated, the spectrum obtained for **2** with 300 μM GNL is comparable to that generated by adding 65 μM PSA (arrows in Figure 1). This is, however, not the case when examined three-dimensionally. While the landscape of **2** obtained with 65 μM PSA (Figure 2g) is less intense than that observed at 300 μM (Figure 2b), its structure and contours remains intact. Even at reduced concentrations this landscaping still serves to distinguish the PSA (Figure 2g) from GNL (Figure 2d).

The combination of a nonridged fluorescence probe **1** and three-dimensional fluorescence spectroscopy provides an efficient means to differentiate subtle structural attributes resulting from molecular interactions. This method was able to distinguish low-affinity protein–carbohydrate interactions ($K_d \sim 10$–50 μM). The ease and technical simplicity of this method suggest a practical means to increase the reliability of affinity matrixes, and illustrate a potent tool for characterizing (or landscaping) a wide-range of biological and chemical processes (e.g. drug screening, characterization of chemical purity, and resolution of mixtures).

In pharmaceutical drug screening low-affinity interactions in the range between 10 μM and 100 μM K_d are currently extremely difficult to measure. As conjugates of **1** and various different classes of ligands including carbohydrates and lipids become screenable, this method will become an increasingly powerful tool for both primary and secondary assays. As seen here, it is not the affinity but the "fingerprint" of molecular recognition which is vital in selecting compounds for cellular and in vivo testing and for establishing structure–activity relationships for follow up bioinformatics, molecular modeling, and/or rational drug design.

Experimental Section

Samples of carbohydrate–lectin mixtures were prepared by adding a DMSO stock solution (20.6 mM) of either **2** or **3** to the appropriate lectins (200 μL, Sigma) in Na_2HPO_4/NaH_2PO_4 (18 mM), $CaCl_2$ (10 mM), $MnCl_2$ (10 mM), NaCl (1 mM), pH 7.2, such that the final carbohydrate and lectin

  1433-7851/01/4010-1890 $ 17.50+.50/0 *Angew. Chem. Int. Ed.* **2001**, *40*, No. 10

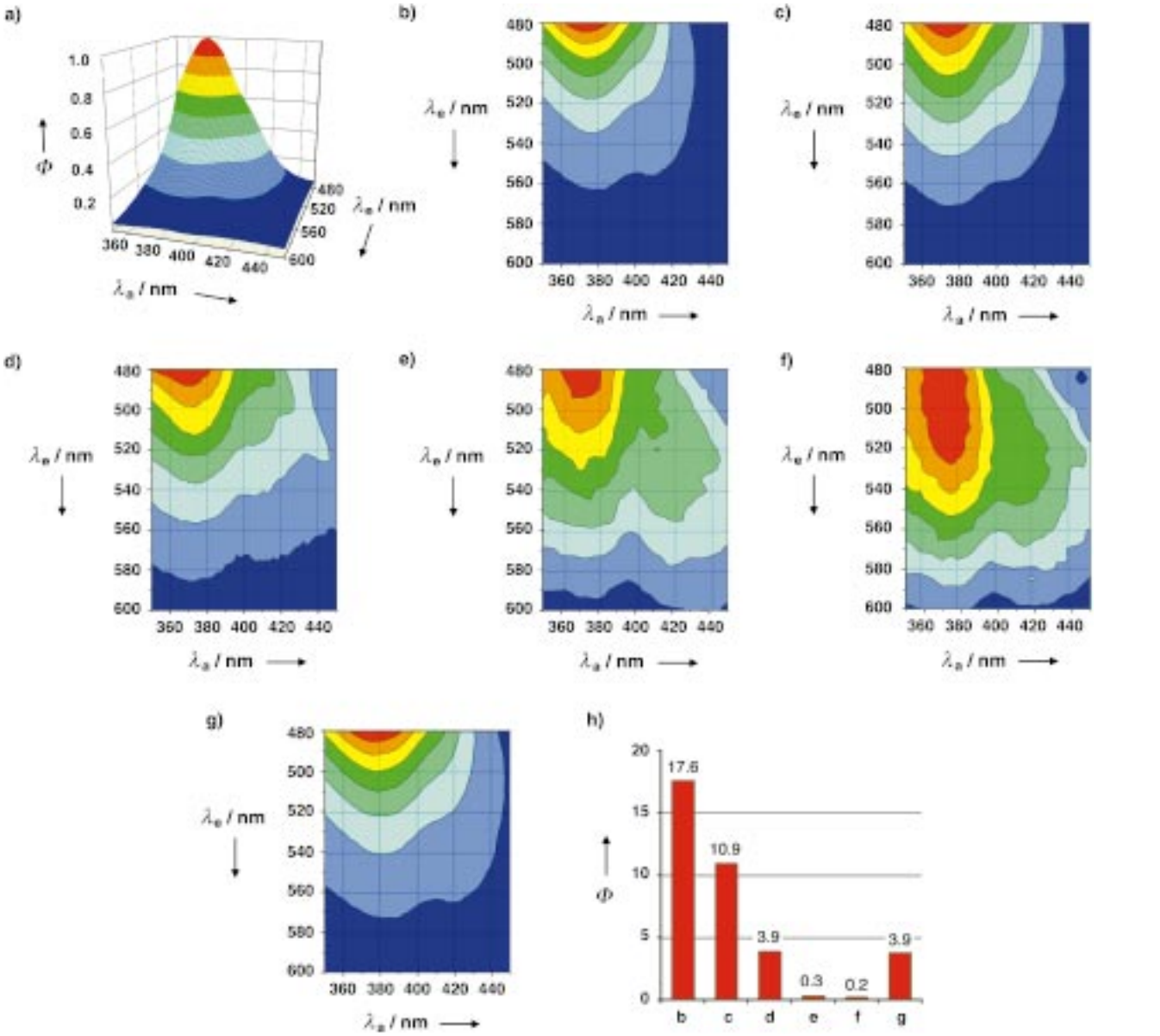

Figure 2. Fingerprint landscapes of the interactions between carbohydrate ligands **2** and **3** and lectins PSA, LCA, and GNL are given by plotting the fluorescent intensity (Φ) against excitation wavelength (λ_a) and emission wavelength (λ_e). [a) three-dimensional diagram, b) contour diagram.] The fluorescence intensity (Φ) is color-coded: 1.0 – 0.875 (red), 0.875 – 0.750 (orange), 0.750 – 0.625 (yellow), 0.625 – 0.500 (green), 0.500 – 0.375 (light green), 0.375 – 0.250 (aqua), 0.250 – 0.125 (blue) and 0.125 – 0 (purple); a) and b) 200 μM **2** with 300 μM PSA, c) 200 μM **2** with 300 μM LCA, d) 200 μM **2** with 300 μM GNL, e) 200 μM **3** with 300 μM LCA, f) 200 μM **3** with 300 μM GNL, g) 200 μM **2** with 65 μM PSA, h) (Φ) observed in (a) – (g) for $\lambda_a = 370$ nm and $\lambda_e = 480$ nm.

concentration was 200 and 300 μM, respectively. These solutions were filtered through a 0.2 μm syringe filter (Millipore) and then transferred to a quartz cuvette (160 μL).

Fluorescence measurements were made in photon-counting mode[13] at 25 °C using magic-angle collection and emission and excitation bandwidths set to 8 nm. The fluorescence intensity for each measurement was standardized against a sample of 5-carboxytetramethylrhodamine. Topologies were collected in three dimensions by monitoring the fluorescence intensity with respect to variance of both excitation and emission wavelengths. Excitation was collected at 2 nm increments of λ_a from 350 to 450 nm with variance of the emission over 5 nm increments of λ_e from 480 to 600 nm. Topologies were then algorithmically corrected using two-pass trinomial smoothing, processed, and displayed graphically.[16]

Received: March 30, 2000
Revised: March 9, 2001 [Z14925]

[1] See: http://www.tirg.org.
[2] a) D. J. Lockhardt, E. A. Winzeler, *Nature* **2000**, *405*, 827 – 836; b) G. Ramsay, *Nat. Biotechnol.* **1998**, *16*, 40 – 44.
[3] a) W. E. Moerner, M. Orrit, *Science* **1999**, *283*, 1670 – 1676; b) S. Weiss, *Science* **1999**, *283*, 1676 – 1683; c) P. Schwille, J. Bieschke, F. Oehlenschlaeger, *Biophys. Chem.* **1997**, *66*, 211 – 228; d) M. Brinkmeier, K. Dorre, K. Riebeseel, R. Rigler, *Biophys. Chem.* **1997**, *66*, 229 – 239.
[4] a) K. S. Lam, *Anti-Cancer Drug Des.* **1997**, *12*, 145 – 167; b) D. Madden, K. Viktor, M. Lebl, *Perspect. Drug Discovery Des.* **1995**, *2*, 269 – 285.
[5] D. R. Walt, *Acc. Chem. Res.* **1998**, *31*, 267 – 278.
[6] a) B. R. Nelson, J.-M. Breguet, *Proc. Int. Soc. Opt. Eng.* **2000**, *4194*, 1 – 197, b) B. R. Nelson, J.-M. Breguet, *Proc. Int. Soc. Opt. Eng.* **1999**, *3834*, 1 – 230, c) A. Sulzmann, B. J. Nelson, *Proc. Int. Soc. Opt. Eng.* **1998**, *3159*, 1 – 234.
[7] a) The SENSI label and its use are described in: a) J. J. LaClair (Scripps Research Institute) US-A 6140041; J. J. LaClair, *Angew.*

  1433-7851/01/4010-1891 $ 17.50+.50/0

Chem. **1998**, *110*, 339 – 343; *Angew. Chem. Int. Ed.* **1998**, *37*, 325 – 329; b) J. J. La Clair, *J. Am. Chem. Soc*. **1997**, *119*, 7676 – 7684.

[8] The photophysics of **1** are further complicated by additional charge transfer states associated with the internal alkyne, see: a) W. Rettig, *Angew. Chem*. **1986**, *98*, 969 – 986; *Angew. Chem. Int. Ed. Engl.* **1986**, *25*, 971 – 988; b) Y. Hirata, T. Okada, T. Nomoto, *Chem. Phys. Lett.* **1997**, *278*, 133 – 138.

[9] LCA is a tetramer composed of two subunits (19874 kDa) of 181 amino acids and two 52 amino acid (5724 kDa) subunits. For crystal structures and sequence information, see: A. Foriers, E. Lebrun, R. Van Rapenbusch, R. de Neve, A. D. Strosberg, *J. Biol. Chem*. **1981**, *256*, 5550 – 5560. Its structure can also be downloaded from the protein databank (PDB) given by 1lem, 1len, 1les, and 2lal.

[10] GNL is a tetramer composed of four identical 109 amino acid (12037 kDa) subunits. For crystal structures and sequence information, see: a) G. Hester, H. Kaku, I. J. Goldstein, C. S. Wright, *Nat. Struct. Biol*. **1995**, *2*, 472 – 479; b) G. Hester, C. S. Wright, *J. Mol. Biol*. **1996**, *262*, 516 – 531; c) G. Hester, C. S. Wright, *Structure* **1996**, *4*, 1339 – 1352. Its structure can also be downloaded from the protein databank given by 1jpc, 1msa, and 1niv.

[11] PSA has a structure comparable to LCA. It is also a tetramer, comprising two 181 amino acid (19969 kDa), and two 52 amino acid (5574 kDa) subunits. For crystal structures and sequence information, see: a) E. J. Meehan, *J. Biol. Chem*. **1982**, *257*, 13278 – 13282; b) G. Gebauer, E. Schilt, H. Rudiger, *Eur. J. Biochem*. **1981**, *113*, 319 – 325. Its structure can also be downloaded from the protein databank given by 1bqp, 1rin, and 2ltn.

[12] Each lectin (GNL, LCA, and PSA) recognizes α-mannopyranosides with affinities ranging from 5 – 100 μM. This includes carbohydrates fused to colorimetric or fluorescent probes through their anomeric center. Typically, the addition of these labels reduces the net affinity of the carbohydrate ligand by an order of magnitude. Based on this assumption, the stoichiometry of lectin to **2** would ensure that at least 80 % of the carbohydrate ligand is bound to the lectin hosts.

[13] Fluorescence measurements were collected on a SLM 8100C Fluorometer equipped with a JD-590 photomultiplier and a 450 W Xenon Arclamp (SLM Instruments).

[14] This difference arose from the structural attributes of these complexes and not from the association or aggregation kinetics of the given complexes. This was verified in that topologies identical to that shown in Figure 2 were also obtained after repeating the measurements after reducing the lectin concentration by 15 %.

[15] BSA does recognize either carbohydrate and therefore serves as a measure of nonspecific interactions. That the fluorescence response from **3** was from nonspecific interactions was further established by comparison with BSA; landscapes generated from addition of **3** either to LCA or BSA were strikingly similar. This result further supports that the fluorescence enhancement with **2** originates, in part, because of docking of the carbohydrate domain in or near the binding pocket of the lectin.

[16] Smoothing was performed using the trinomial algorithm provided within the software package v1995 accompanying the SLM-8100 series 2 spectrometer. The raw data was then processed in Excel97 (Microsoft) and plotted using Origin 5 (Microcal).

Direct Observation of Surface-Controlled Self-Assembly of Coordination Cages by Using AFM as a Molecular Ruler**

Stefano A. Levi, Paolo Guatteri, Frank C. J. M. van Veggel, G. Julius Vancso, Enrico Dalcanale,* and David N. Reinhoudt*

The development of nanotechnology requires miniaturizing complex systems as well as addressing problems at the molecular level.[1] The challenge of overcoming the present limits in routine microfabrication technology in order to reach the nanometer scale requires new methodologies for assembling three-dimensional structures in a controlled fashion directly on solid supports.[2]

In the last few years self-assembly has proven to be a viable alternative to covalent synthesis for the construction of many types of molecular architectures. The desired compounds are formed quantitatively by simply mixing the programmed components under thermodynamic control.[3] Unlike covalent synthesis, self-assembly is a reversible process. This is a very attractive feature because it allows the system to self-repair possible structural deficiencies. Of the self-assembly protocols developed so far, metal-directed self-assembly is particularly appealing as a result of the large number of different structural motifs and bond energies that are available through coordination chemistry.[3a] Until now, the self-assembly approach has mainly been limited to solution chemistry, with very few attempts made to use it directly on surfaces.[4]

Molecular containers represent a very interesting class of compounds[5] as a consequence of their ability to encapsulate ions and neutral molecules. These structures can in principle be addressed individually in a confined environment.[6] Furthermore they are large enough to be detected by scanning force microscopy (SFM).[7] We previously reported the self-assembly of cavitand-based coordination cages formed in solution[8] and the immobilization of covalent container

[*] Prof. Dr. ir. D. N. Reinhoudt, Dr. S. A. Levi, Dr. ir. F. C. J. M. van Veggel
Laboratory of Supramolecular Chemistry and Technology
MESA+ Research Institute, University of Twente
P.O. Box 217, 7500 AE Enschede (The Netherlands)
Fax: (+31) 53-4894645
E-mail: smct@ct.utwente.nl

Dr. E. Dalcanale, Dr. P. Guatteri
Dipartimento di Chimica Organica ed Industriale
Università degli Studi di Parma
Parco Area delle Scienze 17/A, 43100 Parma (Italia)
E-mail: enrico.dalcanale@unipr.it

Prof. G. J. Vancso
Laboratory of Material Science and Polymer Technology
MESA+ Research Institute, University of Twente
P.O. Box 217, 7500 AE Enschede (The Netherlands)

[**] We acknowledge the Nanolink Program of the MESA+ Research Institute (University of Twente), the CNR Nanotechnology Programme, and MURST (Project Molecular Nanoelectronics) for financial support of this work. A special thanks goes to Dr. Maik Liebau (University of Twente) for the preparation of the microcontact-printed substrates and Dr. Frank Geurts (AKZO NOBEL, Central Research Arnhem, NL) for the XPS measurements.

Supporting information for this article is available on the WWW under http://www.angewandte.com or from the author.

  1433-7851/01/4010-1892 $ 17.50+.50/0